


ORIGINAL ARTICLE

A novel pathogenic splice site variation in *STK11* gene results in Peutz–Jeghers syndrome

Na Zhao¹ | Huizhi Wu¹ | Ping Li¹  | Yuxian Wang² | Li Dong¹ | Han Xiao¹ | Changxin Wu¹

¹Institutes of Biomedical Sciences, Key Laboratory of Chemical Biology and Molecular Engineering of National Ministry of Education, Shanxi University, Taiyuan, China

²Department of Obstetrics and Gynecology, The First Affiliated Hospital of Shanxi Medical University, Taiyuan, China

Correspondence

Han Xiao and Changxin Wu, Institutes of Biomedical Sciences, Shanxi University, 92 Wucheng Road, Taiyuan, Shanxi 030006, China.

Email: hanxiao@sxu.edu.cn; cxw20@sxu.edu.cn

Funding information

Shanxi “1331 Project” Collaborative Innovation Center, Grant/Award Number: 206541001

Abstract

Background: Peutz–Jeghers syndrome (PJS) is a rare autosomal dominantly inherited disease resulting in multiple gastrointestinal hamartomatous polyps, mucocutaneous pigmentation, and an increased risk of various types of cancer, and is caused by variations in the serine/threonine protein kinase *STK11* (*LKB1*).

Methods: *STK11* gene variations were identified by analyzing *STK11* cDNA and genomic DNA. Minigenes carrying the wild-type and mutant sequences were subjected to in vitro splicing assay to dissect the features of these mutations. The different distribution of wild-type and mutant protein in cells were tested by Immunofluorescence assays and the functional analysis of the variation were performed using Western blot.

Results: A novel heterozygous splice-acceptor site variation (c.921-2 A>C) in intron 7 of the *STK11* gene which is co-segregates with the PJS phenotypes in the proband and all the affected family members and three previously reported variations (c.180C>G, c.580G>A, c.787_790del) were identified in the four families. The c.921-2 A>C substitution resulted in the inactivation of a splice site and the utilization of a cryptic splice acceptor site surrounding exon 8, generating three different aberrant RNA transcripts, leading to frameshift translation and protein truncation. The results of minigenes indicated that the spliceosome can use a variety of 3' acceptor site sequences to pair with a given 5' donor site. The immunofluorescent visualization showed that the distribution of mutant STK11 was different from that of wild-type STK11, suggesting the mutation may be the causative effect on the dysfunction of the mutant protein. The rescue experiments indicated that the failure of suppressing mTOR phosphorylation by shRNA *STK11* could be eliminated by supply of wild-type *STK11* rather than mutant *STK11*.

Conclusion: We identified a novel heterozygous mutation (c.921-2 A>C) in the *STK11* in a Chinese PJS family. Haploinsufficiency of *STK11* might contribute to the pathogenesis of the disease.

This is an open access article under the terms of the Creative Commons Attribution NonCommercial License, which permits use, distribution and reproduction in any medium, provided the original work is properly cited and is not used for commercial purposes.

© 2021 The Authors. *Molecular Genetics & Genomic Medicine* published by Wiley Periodicals LLC.

1 | INTRODUCTION

Peutz–Jeghers syndrome (PJS, MIM #175200) is a rare autosomal dominant inherited disease characterized by the presence of melanocytic macules of the lips, buccal mucosa and digits; multiple gastrointestinal hamartomatous polyps (Hemminki et al., 1997; Utsunomiya et al., 1975); as well as increased risk of various types of cancers (Hearle et al., 2006; Hemminki et al., 1997, 1998; Jenne et al., 1998; Kuragaki et al., 2003; van Lier et al., 2010; Mehenni et al., 2006; Westerman, Entius, de Baar, et al., 1999; Westerman, Entius, Boor, et al., 1999). The incidence of this disease has been estimated to be ~1 in 8,300 to 1 in 200,000 births (Huang et al., 2015).

Germline mutations in the gene serine/threonine protein kinase 11 (*STK11*, MIM *602216) have been identified thus far as the only cause of PJS (Hemminki et al., 1998; Jenne et al., 1998). *STK11* is located in chromosome 19p13 with 9 coding exons and one non-coding exon and spans about 25 kb in the genome (Masuda et al., 2016). *STK11* haploinsufficiency contributes to the pathogenesis of the disease (Alhopuro et al., 2005; de Leng et al., 2007; Shorning & Clarke, 2016). *STK11* is a tumor suppressor gene and acts as a master regulator in response to stress by direct phosphorylation and activation of a family of AMP-activated protein kinases (AMPKs), which are coupled to nutrient sensing, cell metabolism and cell polarity (Hardie & Carling, 1997; Hawley et al., 2003; Hong et al., 2003; Kottakis et al., 2016; Shackelford & Shaw, 2009; Woods et al., 2003).

The vast majority of human genes are discontinuous in genomic DNA and contain more than one exon. Following transcription, genes expressed as pre-mRNAs are spliced and the intervening introns are removed by spliceosomes with the subsequent joining of the exons to form the mature mRNA that can be translated into a functional protein. Exon recognition is guided by conserved cis-acting elements at the exon-intron boundaries. Defects in alternative splicing can result in a number of human diseases (Hastings et al., 2005).

Minigene construct is a useful and reliable tool for the identification and assessment of the impact of sequence variation on splicing (Cooper, 2005; Li et al., 2019). Expression of minigene pre-mRNAs by transient transfection provides a rapid assay for loss-of-function and gain-of-function analyses of cis-element and trans-acting factors that affect splicing regulation (Cooper, 2005), thereby providing an alternative approach to RT-PCR analysis of patient RNA for the identification of pathogenic splicing defects.

In the present study, we identified a novel splicing variation in a PJS patient in which the penult nucleotide of *STK11* intron 7 changed from A to C. This variation,

c.921-2 A>C, alters the splice site recognition sequence which is crucial for splicing. The aim of this study was to characterize the molecular effect and mechanism of the *STK11* GT-AG intron mutation that causes PJS.

2 | MATERIALS AND METHODS

2.1 | Human subjects

Four PJS patients from four unrelated Chinese families were recruited and peripheral blood samples were collected from them and their family members in EDTA tubes and aliquoted for cryopreservation at -80°C immediately after collection.

2.2 | Immunohistochemistry

The polyp tissue was obtained from the proband (family I) and fixed in 10% formalin solution for 24 hr at 4°C , and then embedded in paraffin for 0.5 hr at 65°C . FFPE samples were prepared for hematoxylin-eosin (HE) staining as previously reported (Chen et al., 2017).

2.3 | Cell culture

HEK293T cells and HeLa cells were purchased from the Cell Bank of the Chinese Academy of Sciences. Cells were cultured in Eagle's DMEM (Life Technologies) supplemented with 10% FBS (BI, Cat. No. 040011A), 1 mM glutamine, 100 U/ml penicillin and 100 $\mu\text{g}/\text{ml}$ streptomycin, 7.5% sodium bicarbonate and 10 mM HEPES (pH 7.5) at 37°C with 5% CO_2 . HEK293T cells and HeLa cells were transfected with plasmids containing either wild-type *STK11* or mutant *STK11* cDNA using polyetherimide (PEI; PolyScience, Cat. No. 23966-2) according to the manufacturer's instructions, then incubated for 24–48 hr before use.

2.4 | Detection of *STK11* germline mutations

Genomic DNA was extracted using the DNeasy Blood & Tissue Kit following the manufacturer's protocol (Qiagen, Cat. No. 69506). PCR was performed to amplify the nine coding exons along with the flanking introns of the *STK11* gene (NC_000019.10, NM_000455.5) with specific primers as previously described (Jenne et al., 1998). Sanger sequencing was performed using the 3730xL DNA analyzer (Sangon Biotech) and analyzed using the Sequencing Analysis 3.0 software (Applied Biosystems).

2.5 | In silico mutation analysis

We predicted the effects of *STK11* variations on the protein function using several bioinformatics tools, including SIFT (<http://provean.jcvi.org/index.php>), Mutation Taster (<http://www.mutationtaster.org/>), and Polyphen-2 (<http://genetics.bwh.harvard.edu/pph2/>).

2.6 | Analysis of cDNAs from endogenous *STK11* mRNAs

Peripheral blood samples were incubated with 200 μ l 1 mg/ml puromycin for 6 hr as described previously (Chen et al., 2017) before total RNA was isolated using Trizol (Invitrogen, Cat. No. 15596-018). cDNA was synthesized by reverse transcription of isolated RNA using 5x All-In-One Mastermix Kit (ABM Cat. No. G492) for RT-PCR and PrimeScript™ RT reagent Kit (Takara Cat. No. RR037A) for qRT-PCR. RT-PCR was performed using primers pair of *STK11* minigene (Table 2) to obtain the PCR products spanning exons 6 and 8.

2.7 | Minigene construction

STK11 wild-type or mutant minigenes encompassing exon 6, intron 6, exon 7, intron 7 and exon 8 of the *STK11* gene were constructed by amplification with genomic DNA from the healthy control III-3 or affected patient II-3 using PrimeSTAR® GXL DNA Polymerase, respectively (Takara, Cat. No. R050Q). The amplified fragments were digested with Xho I (Takara Cat No. 1094S) and EcoR I (Takara Cat. No. 1040S) and then subcloned into the multicloning sites of the pEGFP-C3 vector using Xho I and EcoR I restriction sites. Minigene constructs were validated (with PCR products from exon 6 to exon 8) by Sanger sequencing analysis with the universal primer (5'-TATGTTTCAGGTTTCAGG-3'; Sangon Biotech).

2.8 | Plasmid construction

The *STK11* gene was constructed by amplification with cDNA from HEK293T cell using PrimeSTAR® GXL DNA Polymerase (Takara, Cat. No. R050Q). The amplified fragments were digested with Xho I (Takara Cat No. 1094S) and EcoR I (Takara Cat. No. 1040S) and then subcloned into the multicloning sites of the pEGFP-C3 vector named GFP-STK11-WT. The plasmid GFP-STK11-rWT and GFP-STK11-rMT were constructed with site-directed mutation using the primers in Table 1 and GFP-STK11-WT.

2.9 | In vivo splicing analysis of *STK11* minigenes

Minigene constructs were transfected into HEK293T cells cultured with Dulbecco's modified eagle medium (DMEM, Cellmax Cat. No. CGM102.05) containing 10% FBS (BI, Cat. No. 040011A), 100 U/ml penicillin and 100 μ g/ml streptomycin (Transgen Biotech, Cat No. FG101). To generate transient expression of *STK11* in HEK293T cells, the mixture contains 3 μ g wild-type or mutated *STK11* plasmids and 9 μ l PEI (Polyscience, Cat. No. 23966-2) in 200 μ l serum-free DMEM medium was transfected HEK293T cells at 50% grown confluence in six-well plates. After 4–6 hr incubation at 37°C with 5% CO₂, the cells were subsequently cultured in DMEM supplemented with 10% FBS and incubated for 24 hr in the incubator.

2.10 | mRNA quantification

Total RNA was isolated from the HEK293T cells using Trizol reagent (Invitrogen, Cat. No. 15596-018). cDNA was synthesized using PrimeScript™ RT reagent Kit (Takara Cat. No. RR037A). The mRNA levels of *STK11* and *GAPDH* were quantified by quantitative reverse transcription PCR (qRT-PCR; Roche LightCycler 480 II) using SYBR Green (Transgen Biotech, Cat. No. A6001) and the primers are listed in Table 2. Relative expression of mRNA level was assessed using the comparative Cq method. All of the measurements were normalized based on the endogenous *GAPDH* mRNA level.

2.11 | The plasmids for lentiviral shRNA

STK11 shRNA sequences (5'-GATCCGCCAACGTGAAG AAGGAAATTTCAAGAGAAATTCCTTCTTCACGT TGGCTTTTTGCTAGCG-3' [Pena et al., 2015], underlines indicate complementary 21-bp stem sequences corresponding to *STK11* cDNA sequence) were cloned into pSIREN-RetroQ vector using EcoR I and BamH I sites (Addgene Cat. No. 25788).

Lentiviruses were produced in HEK293T cells after co-transfection of lenivirus plasmid vector, psPAX and pMD2.G at the ration of 5:5:1 using Polythermide (PEI; PolyScience, Cat. No. 23966-2). After 48 and 72 hr, the medium containing lentivirus were collected, centrifuged at 1000 \times g, and filtered through a 0.22 μ m filter. Cells were transduced with the medium and normal medium at the ratio of 3:1 and selected with puromycin (1 mg/ml) after 72 hr for 7–10 days.

TABLE 1 Primers for amplification and sequencing of the *STK11* gene

Primer	Forward (5'-3')	Reverse (5'-3')	Base	Remarks
Exon 1	GGTCCCCGAGGACGAAAGTTGA	ACCATCAGCACCGTGACTGG	679bp	Dieter.
Exon 2	TCGCCGGCCGATGACAGA	AAGGAGACGGGAAGAGGAGCAG	413bp	Dieter.
Exon 3	GAGGAGGGCAAGGTGGGT	GTGTGGCCTCACGGAAGGAG	283bp	Dieter.
Exon 4-5	AGCTGGCCCTGTGGTGTITG	CAGAGGCCCTCGGAGTGTG	503bp	Dieter.
Exon 6	GCCTCTGTCCCTGGGGTAGA	TCAGTCCTCTCAATGCCTGCTG	340bp	Dieter.
Exon 7	GCGGGGTCCCCCTTAGGAG	CTAGCGCCCGCTCAACCAG	264bp	Dieter.
Exon 8	GGAGCTGGTCCGAAAACCTGGA	TGCTCCCGTGGGACATCCTG	321bp	Dieter.
Exon 9	GTAAGTGGTCCCGTGGTG	GTGGCATCCAGGCGTGTCC	357bp	Dieter.
qPCR	CGGCAGCACAGCTGGTTC	CGGGCACCGTGAAGTCTT	199bp	
STK11 minigene	CCGCTCGAGCGGATGCTACAACATCACACCGGGTC	CCGGAATTCCGGCGGGCACCGTGAAAGTCCTG	C:378bp G:1964bp	
STK11 Whole	GCGCTCGAGCTATGGAGGTGGTGGACCCGC	GCGGAATTCTCACTGCTTGCAGGCCCG	1302bp	
STK11 IVS7	CCGGCAGATCCGGCAGCACAG	GGAGGATGTTTCTTCCGGAAACCAG	6000bp	
STK11 C3	CTGGTCCGGAAACAATCCTCC	CTGTGCTGCCGGATCTGCCCG	6000bp	
shSTK	GATCCGCCAACGTGAAGAAGGAAATTTTCAAGAGAAATT TCCCTTCTCACGTTGGCTTTTGTAGCG	AATTCCGTAGCAAAAAGATCCTCAAGAAGAAGAAAGTTTCTCT TGAAAACTTCTTCTTCTTGAGGATCG	-	Pena et al
shSTKre1	AGGCTAACGTTAAGAAAAGAAATACAACACTACTGAGGAGGT TACGGC	GTTGTATTCTTTCTTAAACGTTAGCCTCCCCGTTGGGGATCCTTC	6000bp	
shSTKre2	AGGCTAAGGTTAAAAAAGAGATACAACACTACTGAGGAGGT TACGGC	GTTGTATcTCTTTTAAcTTAGCCTCCCCGTTGGGGATCCTTC	6000bp	

The first 8 primers in the table were used to amplify the exons of *STK11* gene (*NC_000019.10, NM_000455.5*) and sequencing. The primer of qPCR were used to quantify mRNA. The primer of *STK11 IVS7* and *STK11-C3* were used to construct p-EGFP-C3-WT plasmid using homologous recombination. The primer of shSTK was used to construct pSIREN-RetroQ-stk11-shRNA which was used to knockdown the endogenous *STK11*. The primer of shSTKre1 and shSTKre2 were used to construct the plasmids that transfected the knock down cells which exclusive the knock down sequence.

TABLE 2 Clinical manifestations of patients with PJS

Family	Patient	Gender	Age	Mucocutaneous pigmentation	Distribution of polyps	Laparotomy
Family-1	II-3	M	35	Yes	SB, CR	Yes
Family-1	III-5	M	5	Yes	SB, CR	Yes
Family-2	II-4	F	49	Yes	SB, CR	Yes
Family-3	I-2	M	36	Yes	ST, SB, CR	Yes
Family-3	II-2	M		Yes	ST, SB, CR	Yes
Family-4	III-1	F	27	Yes	ST, SB, CR	Yes
Family-4	III-2	F	23	Yes	ST, SB, CR	Yes

Abbreviations: CR, colorectum; F, female; M, male; SB, small bowel; ST, stomach.

2.12 | Western blot analysis

Cells were washed twice with PBS and then either scraped in RIPA lysis buffer containing protease inhibitors (Solarbio, Cat. No. R0020) or lysed in 1× SDS loading buffer. Cell lysates were incubated on ice for 30 min and then sonicated for 10 s. The soluble fraction was then isolated by centrifugation at 13,000×g for 15 min at 4°C. Total protein concentration was measured using a Pierce™ BCA protein assay kit (Thermo). Proteins in the lysates were separated by electrophoresis in a 10% SDS-PAGE gel and transferred to a polyvinylidenedifluoride (PVDF; GE, Cat. No. A10178786) membrane. The membrane was blocked in 5% milk (BD Biosciences, 4335762) for 1 hr and then immunoblotted with antibody overnight at 4°C. After washing three times (5 min every time) with TBST buffer, the membrane was then incubated with secondary antibody for 2 hr at room temperature. Quantitation was performed using Odyssey CLX (Li-COR) and Amersham Imager 600 (GE Healthcare). The following antibodies were used: THETM GFP rabbit polyclonal antibody (GenScript, Cat. No. A01704-100), mTOR(S2442) polyclonal antibody (Bioworld, Cat. No. BS3611), mTOR(phospho-S2448) polyclonal antibody (Bioworld, Cat. No. BS4706), Beta actin Polyclonal antibody (Absin, Cat. No. abs132001), THETM alpha Tubulin monoclonal Antibody (GenScript, Cat. No. A01545), 4E-BP1 (53H11) rabbit monoclonal antibody (Cell Signaling, Cat. No. 9644T), Phospho-4E-BP1 rabbit monoclonal antibody (Thr37/46; 236B4; Cell Signaling, Cat. No. 2855T), p70 S6 Kinase (49D7) rabbit monoclonal antibody (Cell Signaling, Cat. No. 2708T), Phospho-p70 S6 Kinase rabbit monoclonal antibody (Ser371; Cell Signaling, Cat. No. 9208T).

2.13 | Immunofluorescence analysis

HeLa cells grown on coverslips were fixed by 4% paraformaldehyde at 37°C for 10 min. Before staining by

DAPI (Sigma), cells were permeabilized with 0.5% Triton and X-100 for 5 min, then mounted on glass slides using gelvatol. Images were captured using a Delta Vision Image Restoration Microscope with a ×63 objective (DeltaVisionElite, GE).

2.14 | Statistical analysis

All data are presented as the mean ± SD from at least three separate experiments. The *p*-values were determined by the two-tailed Student's *t* test. *p* < .05 was considered as statistically significant.

3 | RESULTS

3.1 | Family pedigree/patient information

All recruited patients (Figure 1) exhibited common signs of PJS, including multiple gastrointestinal hamartomatous polyps and mucocutaneous pigmentation. Clinical manifestations of the patients with PJS are shown in Table 2. The blood samples from four unrelated Chinese families (Figure 1) were obtained for genomic DNA or total RNA extraction. Sanger sequencing was performed for all the exons and exon–intron splice junctions of the *STK11* gene (NC_000019.10, NM_000455.5; primers shown in Table 1). Four different heterozygous mutations were identified. Among these variations, c.580G>A was a missense mutation in exon 4 and resulted in amino acid substitution of Asp194Asn, and c.787-790del was an indel in exon 5 causing a reading frameshift and resulted in a truncated STK11 protein (p.Phe264Argfs*22). c.180C>G was a non-sense mutation in exon 1 and resulted in a truncated STK11 protein p.Tyr60*. A novel variation c.921-2 A>C is a single-base substitution located in intron 7 that was predicted to be the putative splicing site using Mutation Taster (<http://www.mutationtaster.org/>), and we speculated it might affect

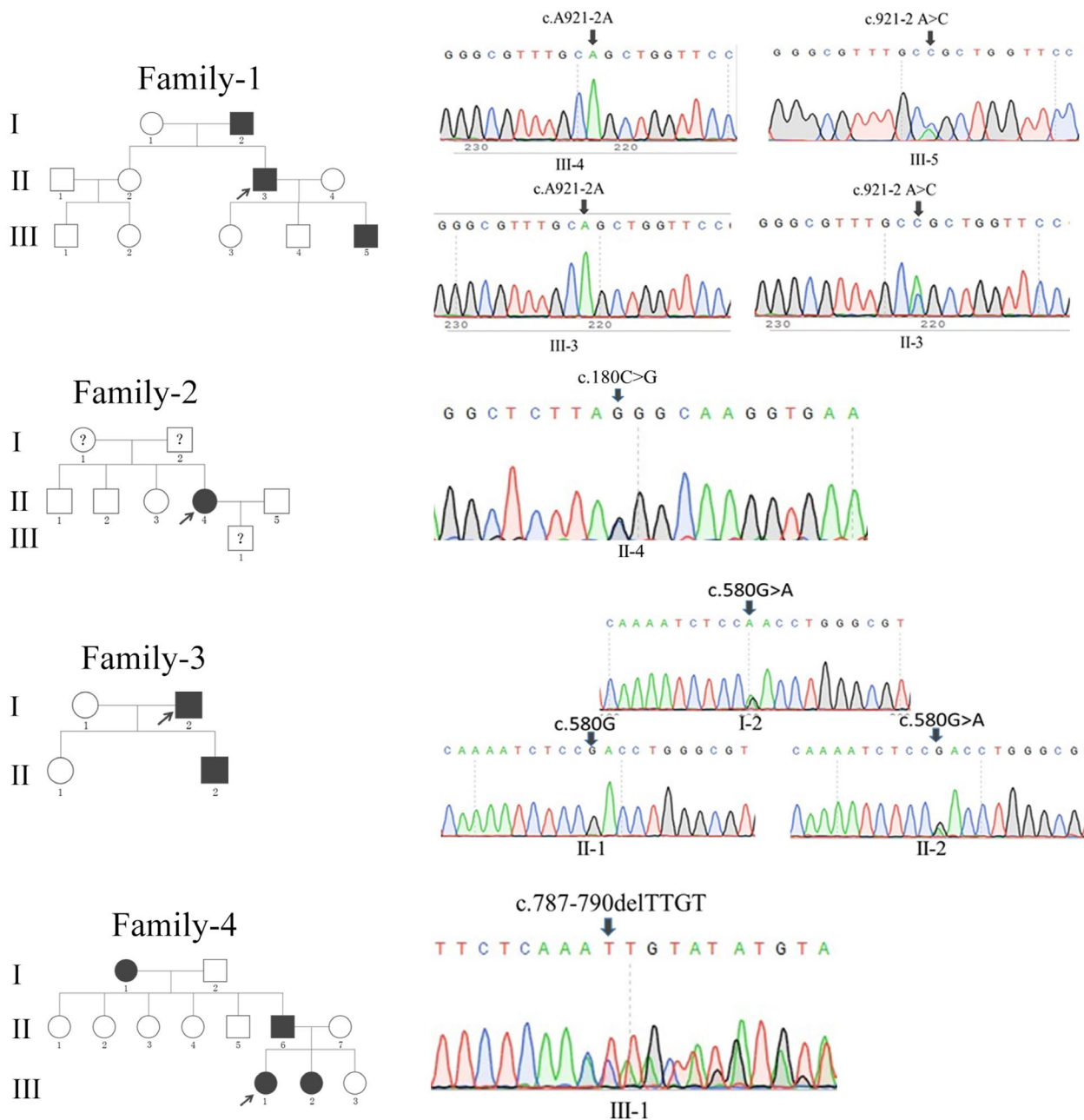


FIGURE 1 Family pedigree of PJS. Family pedigree and Sanger sequencing analysis. Squares indicate males, circles indicate females, blackened symbols denote affected individuals. The proband is indicated by arrows (↗)

the splicing of *STK11*. To validate the novel mutation, we sequenced exon 8 and the junctions of *STK11* in other family members from family I. The c.921-2 A>C variation was only found in affected individuals but not unaffected family members (Figure 1). In addition, it was predicted to be disease-causing by in silico analysis using Mutation Taster (with a *p* value of 1), suggesting a high possibility of functional alterations of the translated protein. Therefore, the novel variation c.921-2 A>C in intron 7 is likely the cause of PJS in family I.

3.2 | Splicing defect in *STK11* c.921-2 A>C PJS patients

We sought to elucidate the mechanism underlying that the c.921-2 A>C variation affects *STK11* expression and causes PJS. The polyp tissue (Figure 2a) from the gastrointestinal track was obtained from the proband of family I and prepared for hematoxylin-eosin (HE) to visualize the microstructure of the polyps. Pathological sections displayed the muscle fibers of the muscularis mucosae in the form of a dendritic structure

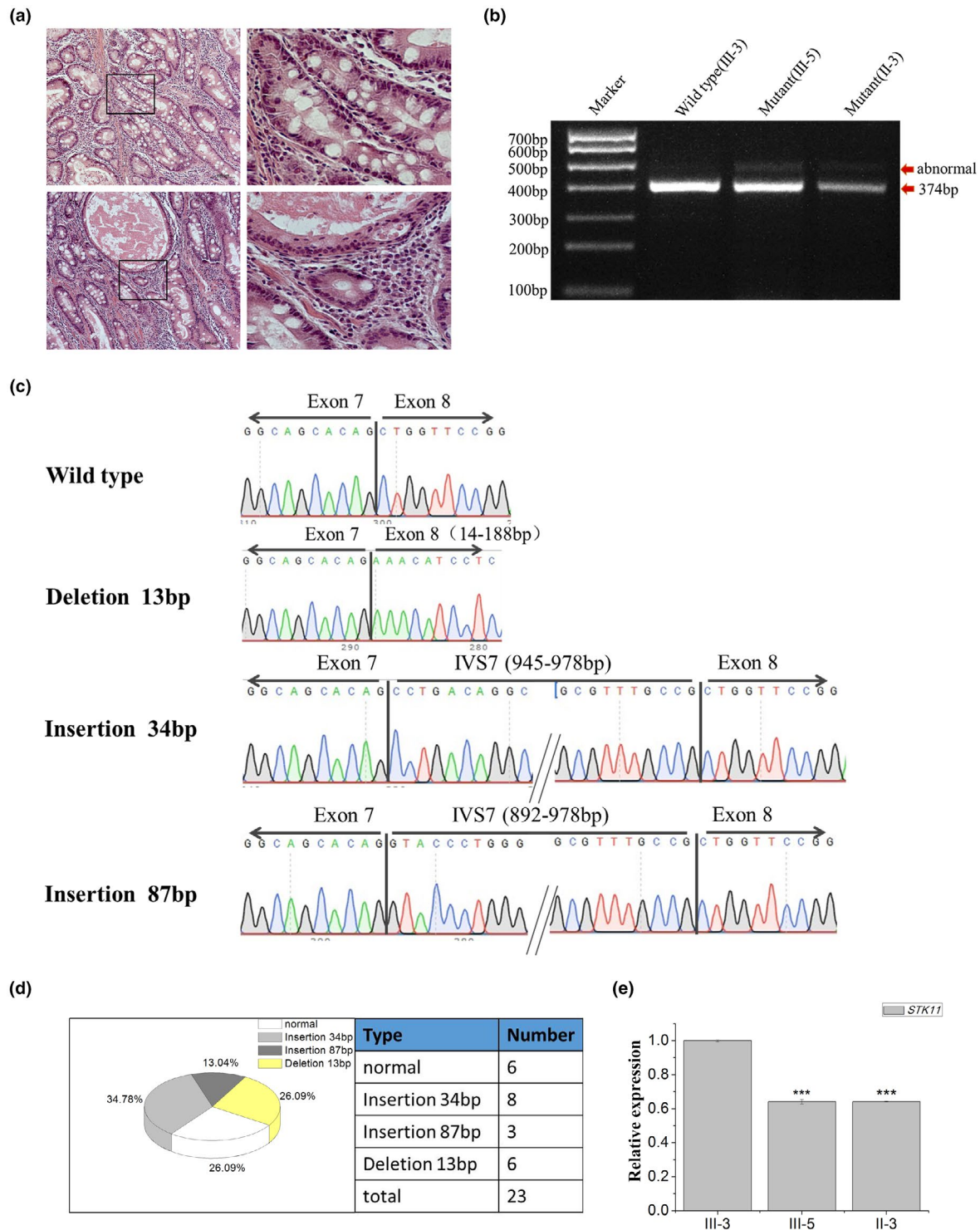


FIGURE 2 Alternative splicing of *STK11* (NC_000019.10, NM_000455.5; c.921-2 A>C; a) Staining of tissue section from patient with PJS. HE staining of a colon hamartomatous polyp obtained from the patient II-2 in Family A. (b) RT-PCR analysis of endogenous *STK11* RNA from unaffected family member (III-3) and PJS patients (III-5, II-3). (c) Sanger sequencing analysis for the alternative splicing products. The sequence of the upper band in figure B reveals two kinds of insertion and a deletion at the junction between exons 7 and 8 of the *STK11* cDNA compare to wild type. (d) Statistical analysis of the numbers and types of the cDNA clones that sequenced. (e) qRT-PCR analysis performed on total RNA obtained from blood cells of patient II-3, III-5 and healthy control $p < .001$. Levels were normalized to the amount of actin. Data represent the mean \pm SE of three independent measurements performed in triplicate

(Figure 2a). Splicing defect often results in the production of aberrant mRNA transcripts (Figure 2b). To evaluate the mRNA profile associated with the c.921-2 A>C variation,

we performed RT-PCR of the region spanning exons 6–8 (Figure 2b). In the control sample from III-3, only one band could be detected and corresponded to the full-length mRNA

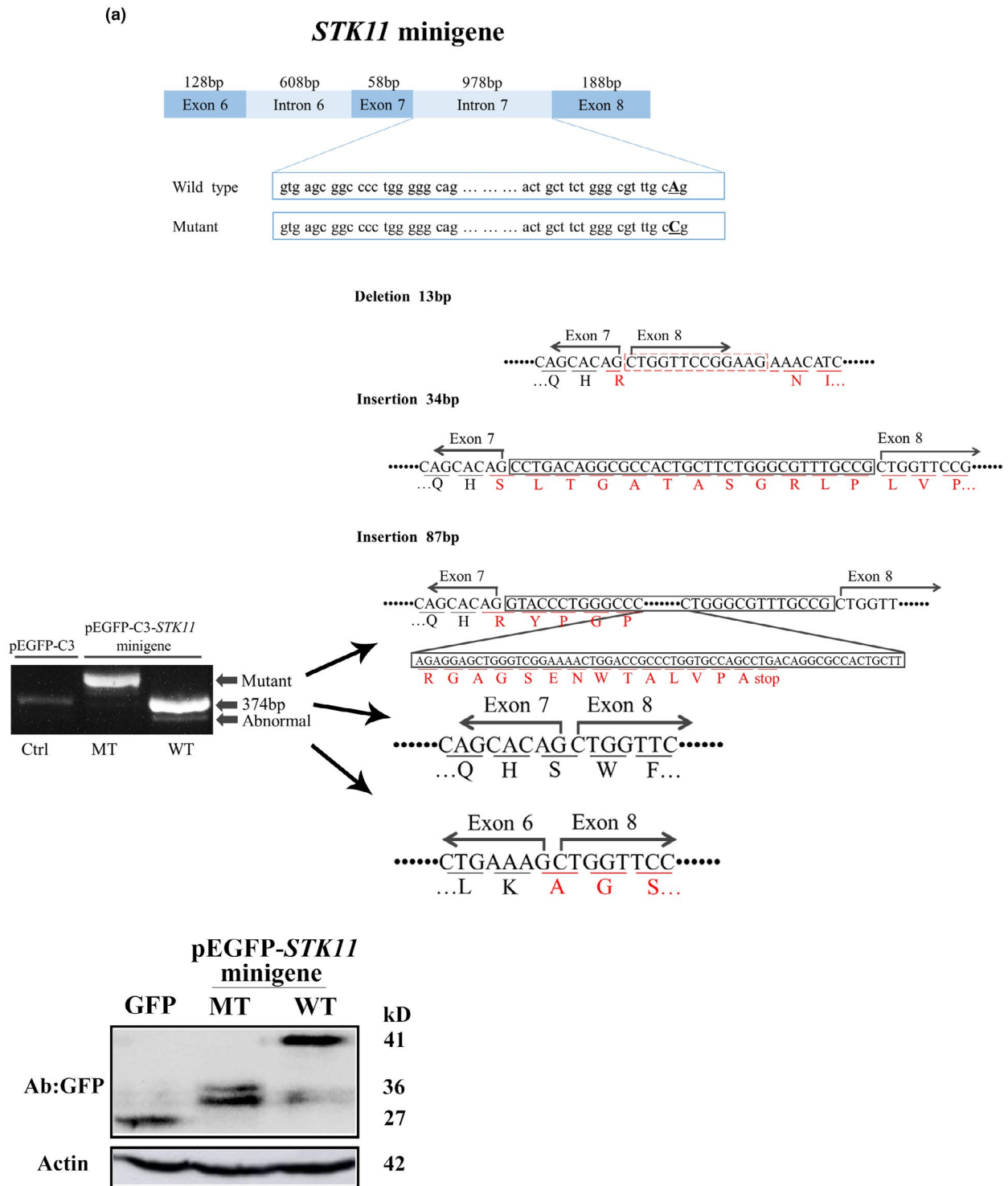


FIGURE 3 Aberrant spliced products arise from *STK11* c.921-2 A>C mutation. (a) Schematic representation of the *STK11* minigene constructs, covering the region from exon 6 to exon 8. The nucleotide change in intron 7 of both wild-type and mutant *STK11* constructs are highlighted. The changed nucleotide in intron 7 of both wild-type and mutant *STK11* minigene are labelled by underscore and capital. (b) Minigene in vitro splicing assay. *STK11* minigenes harboring the wild-type or mutant *STK11* was transiently transfected into HEK293T cells. The splicing products were visualized by RT-PCR and DNA gel electrophoresis. The aberrant transcript identity was analyzed by Sanger sequencing as described. The aberrant transcript products generated by minigene harboring *STK11* c.921-2 A>C variation are represented as figure B. (c) Western blot analysis for the expression of the wild-type and mutant minigenes. Whole cell lysates were separated by SDS-PAGE and probed with GFP monoclonal antibody

transcript. In contrast, in patients III-5 and II-3, we detected a major peak corresponding to the full-length mRNA and a minor upper peak. This result indicated that the variation c.921-2 A>C affected the transcription of *STK11*.

To clearly define the identity of the spliced transcripts, we extracted the spliced products and amplified by RT-PCR from the gel and subcloned them into a sequencing vector. Twenty-three cDNA clones from the PJS patient II-3 were sequenced. Among all the sequenced clones, six clones were wild-type cDNAs, presumably originating from the normal *STK11* allele. Three different abnormal transcripts might be caused from the variation of c.921-2 A>C were detected. One deletion with 13 bp from exon 8 close to the 5' terminal (p.Ser307Argfs*24) and two insertions with 34 bp (p.Trp308Leufs*20) and 87 bp (p.Ser307Argfs*19) from intron 7 respectively, were identified (Figure 2c,d). The insertion and deletion in cDNA could cause defected STK11 protein.

Total RNAs isolated from peripheral blood cells of patients and control subjects were quantified to evaluate the amount of *STK11* transcripts. We used qRT-PCR to quantify *STK11* transcription levels in peripheral blood cells of PJS patients and control subjects. mRNA levels of *STK11* were remarkably reduced in patient III-5 and II-3 compared to the control III-3, showing that the level of normal *STK11* mRNAs in patients were lower than that in the healthy subjects (Figure 2e).

3.3 | Splicing defect confirmation by hybrid minigene splicing assays

To confirm that the aberrantly spliced *STK11* transcripts from patients are derived from the c.921-2 A>C variation, we constructed minigenes (Figure 3a) composed of exon 6, intron 6, exon 7, wild-type intron 7 or mutant intron 7 containing c.921-2 A>C, and exon 8. Minigene constructs were validated by Sanger sequencing and then transfected into HEK293T cells. Immunofluorescence results showed that the plasmid transfection was successful (Figure S1a). Forty eight hours after transfection, total RNA was extracted and RT-PCR was performed using *STK11* primers (as shown in Table 1). PCR products were separated by DNA electrophoresis and different isoforms were excised from 2% gel and identified by sequencing. In control HEK293T cells, a weak band was shown which represented the endogenous full-length *STK11* minigene mRNA (E6+E7+E8; Figure 3b). In cells transfected with the wild-type construct, a very strong band of 374bp in length was seen which represented the wild-type full-length *STK11* minigene mRNA (E6+E7+E8). In contrast, a larger band arose from the c.921-2 A>C minigene construct was found in the mutant transfected cells which are consistent with the results from the patient's blood (Figure 2c, sequencing data not shown).

Unexpectedly, we observed a weak band slightly smaller than 374 bp band in wild-type minigene transfected cells (Figure 3b). We reasoned that it might arise as a result of polymorphism as the minigene constructs were derived directly from genomic DNA products. Accordingly, we sequenced the minigene construct and found several polymorphic sites (Table S1). When we reverted these sites into the respective wild-type sequences, we still observed a weaker band smaller than the 374 bp band which lack of exon 7 (Figure S1b). Therefore, polymorphism was not responsible for the presence of the detected weaker band.

We further performed Western blot analysis to investigate the protein expression from the minigenes. In pEGFP-C3-transfected cells, a strong band at the molecular weight of ~27 kD was observed, which represented GFP (Figure 3c). In wild-type minigene-transfected cells, a band of 41 kD in weight was seen which represented the fusion protein of GFP with STK11 (E6 + E7 + E8). In contrast, in c.921-2 A>C mutant minigene-transfected cells, several bands of ~36 kD in weight were seen that represented the truncated fusion protein arising from the aberrant mRNA transcripts, which was consistent with the results of our alternative transcript analysis. Western blot of minigene showed that the mutation cannot generate a correct STK11 protein product instead, its products were three abnormal polypeptides, almost 9 kD. Only two abnormal polypeptides were observed in Western blot analysis which might due to the difference of molecular weight is too small to separate by 15% SDS-PAGE (Figure 3c).

3.4 | Analysis of STK11 mutation

To confirm whether variation in the *STK11* gene from patient II-3 in family I has influenced the function of the STK11 protein, we constructed two plasmids included the whole *STK11* gene and intron 7 using homologous recombination (Figure 4a). Through sequence alignment, we found the c.921-2 A>C variation caused a translational frameshift, and a premature stop codon appeared downstream of the codon 308 of STK11 (p.Trp308Leufs*20, p.Ser307Argfs*19, p.Ser307Argfs*24), which caused about 102-amino-acid-residue change and partial loss of C-terminal domain (Figure 4b). This mutation results in three truncated proteins lacking the C-terminal, resulting two bands of size of about 36 kD proteins. Evolutionary conservation analysis of amino acid residues showed that these impaired amino acid residues were most highly evolutionary conserved among STK11 from different species, indicating the variation most likely predisposed to PJS (Figure 4b). From the structure diagram (Figure 4c) of STK11 wild-type protein and mutant protein, it showed that the mutant protein had the whole NRD domain, NLS sequence, and almost Kinase domain, but no CRD domain. The deficiency of CRD domain may influence the function of the STK11 protein.

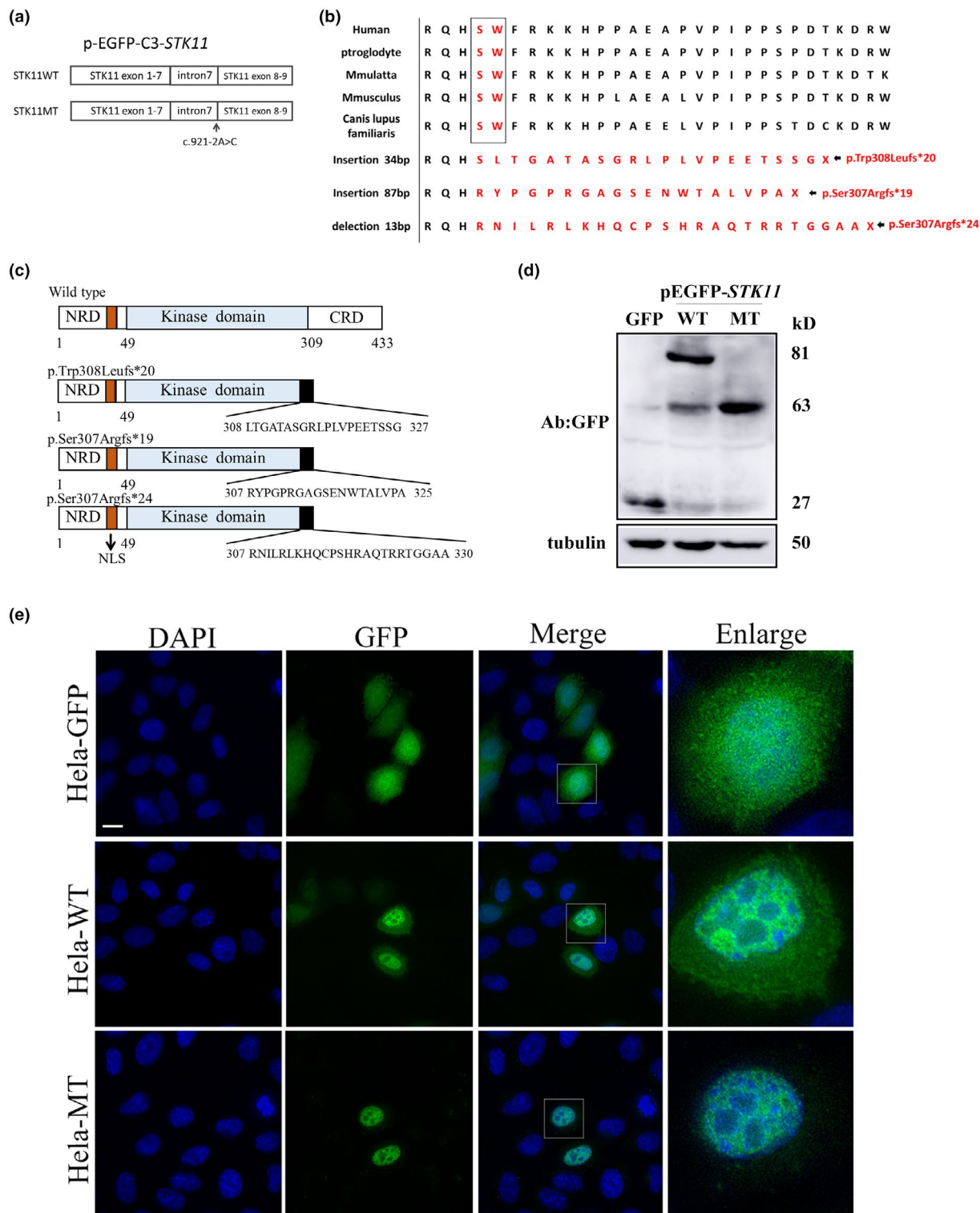


FIGURE 4 Analysis of STK11 variation (a) Schematic representation of the STK11 constructs, covering the region of the whole CDS region and intron 7. The nucleotide change in intron 7 of both wild-type and mutant STK11 constructs are signed below. (b) Evolutionary conservation of amino acid residues altered by c.921-2 A>C across different species. (c) Schematics of the secondary structure or functional domains of the STK11 protein including the wild-type and mutant (p.Trp308Leu fs*20, p.Ser307Arg fs*19, p.Ser307Arg fs*24). (d) The expression of the STK11 protein in HEK 293T cells transfected with GFP alone, wild-type and mutant STK11. (e) HeLa cells were transfected with GFP alone, GFP-STK11-WT and GFP-STK11-MT plasmids and the localization of wild-type and mutant STK11 were studied by immunofluorescence. Bar: 15 μ m

To understand whether the mutant can produce a normal STK11 protein, we examined the protein using Western blot. The results showed that the mutation resulted in an abnormal product with the molecular weight about 63 kD compared with the wild-type about 81 kD (Figure 4d).

To identify whether the mutant STK11 has altered its distribution in transfected cells, we transfected STK11-wild-type and STK11-mutant with GFP-tag into HeLa cells. In GFP alone transfected cells, GFP signal was detected in both nucleus and cytoplasm equally, in GFP-STK11-WT transfected cells, the STK11-GFP fusion protein was expressed both in the nucleus and cytoplasm, but most of the fusion protein was in nucleus and less fusion protein in cytoplasm. Surprisingly, much less GFP fusion mutant was observed in cytoplasm of GFP-STK11-MT

transfected cells (Figure 4e). Under normal physiological conditions, STK11 is located in the nucleus but it will transfer into the cytoplasm when it functions as a kinase that phosphorylate AMPK (Lizcano et al., 2004). The alteration in the distribution of GFP-STK11-MT may be one of the reasons for its dysfunction.

3.5 | Function analysis of STK11 mutation

To further analyze whether the mutant still retained some function of the wild-type STK11 protein, we generated a stable STK11 knockdown HEK293T cell line using transfection and transformation of a lentiviral system encoding *STK11* shRNAs. The efficiency of STK11 knockdown was

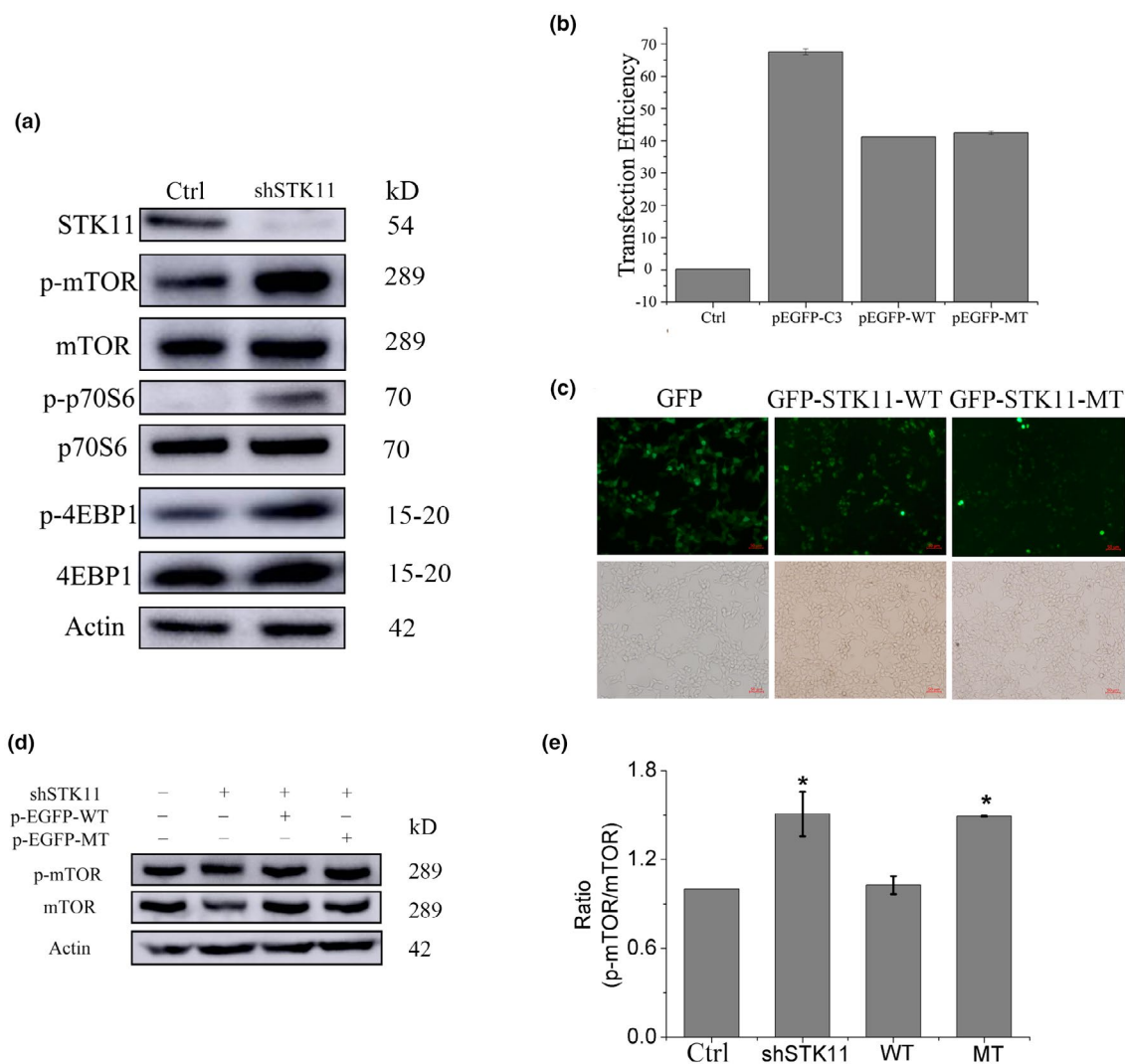


FIGURE 5 Function Analysis of STK11 variation (A) Western blot of immortalized HEK293T cells stably transduced with lentivirus encoding STK11shRNA and untransduced HEK293T cells show the efficiency of STK11 knockdown, and modest effects on the levels of the phosphorylated forms of downstream mTOR-signaling components p70S6 or p4EBP1. (b) The transfection efficiency of the rescued transfection. (c) Images taken from bright and fluorescence fields were used to show successful transfection of rescue plasmids GFP, GFP-STK11-WT or GFP-STK11-MT plasmids in shSTK11-HEK293T cells. Bar: 50 μm (d,e) The phosphorylation of p-mTOR in transfected the STK11 knockdown cell line with GFP alone, GFP-STK11-WT and GFP-STK11-MT rescue plasmids. The *p* value of shSTK11 was .042, and the *p* value of MT was .014

quantified using Western blotting by comparison its STK11 endogenous expression in HEK293T cell line (Figure 5a). As expected, STK11 knockdown resulted in high levels of mTOR phosphorylation (at Ser2448), p-p70S6K(Ser371), p-4EBP1(Thr37/46), which are downstream components of the AMPK/mTOR pathway. After STK11 knocking down in HEK293T cells, transfection with either plasmid GFP-STK11-rWT expressing recombinant wild-type STK11 (rWT-STK11) or GFP-STK11-rMT expressing recombinant (rMT-STK11) was performed to rescue the phosphorylation of mTOR. Flow cytometry showed that the transfection efficiency of those two plasmids was similar (Figure 5b), but the visualization of transfection showed that the fluorescence intensity of cells expressing rWT STK11 was much stronger than that of the rMT STK11 expressing cells (Figure 5c). Western blot showed that the phosphorylation of mTOR (at Ser2448) was rescued in rWT STK11 transfected but not in rMT STK11 transfected cells which were STK 11 absent (Figure 5e). It seems that the patients cannot produce enough amount of a normal STK11 protein due to the mutation c.921-2 A>C which is a heterozygous mutation causing half mRNA expression of wild-type *STK11*, and half mRNA expression of mutant *STK11* which yielded STK11 with N-terminal non-catalytic domain and large party of catalytic kinase domain, losing CRD domain, and so dysfunctional.

4 | DISCUSSION

PJS is a dominantly inherited disorder with nearly complete penetrance in patients with variation in the *STK11* gene (Yoo et al., 2002). Currently, 511 mutations in *STK11* have been detected in patients with PJS or other disorders (HGMD Professional 2019.1). The STK11 protein is composed of three major domains: the N-terminal non-catalytic domain (encoded by amino acids 1–49), the catalytic kinase domain (encoded by amino acids 49–309) and the C-terminal non-catalytic regulatory domain (encoded by amino acids 309–433; Hanks et al., 1988). Variations in PJS patients are mostly located in the catalytic domain region and cause dysfunction in kinase activity, thus disrupting the function of STK11 (Huang et al., 2015).

The production of mature RNA requires the precise removal of intervening intronic sequences by spliceosome. Pre-mRNA splicing is mediated by conserved but yet degenerate cis-acting signal sequences at the splicing sites (Hastings et al., 2005). The most common results of splicing variation are exon skipping, and also cryptic splice site activation. In our study, we detected a novel variation located in intron 7 between exon 7 and exon 8 which gene locus (HGMD number: CS035538; c.921-2 A>G) had been reported (Kottakis et al., 2016). However, in contrast

to the previous report of A>G transition, our proband carried an A>C transversion. In our case we found the spliceosome utilized cryptic splice acceptor site located in intron 7. All of the aberrantly spliced products identified in our study introduce premature termination codons. Therefore, STK11 is thought to lose its kinase activity due to the truncated protein product, leading to the development of the PJS.

Furthermore, in silico tool analysis showed that a cryptic splice acceptor site located at several positions, in consistency with our in vitro minigene splicing assay.

However, our minigenes were with the products from the patients, inevitably there were some polymorphic sites belong to the patients involved in the minigene despite in wild-type and mutant. They were predicted to be polymorphic sites with a high population carriage by Mutation Taster. After transfection with the minigene into HEK293T cells, one or two polymorphic sites involved in the wild-type minigene could generate an abnormal mRNA which loses 67 bp (data not shown here) compared with the normal. The polymorphic sites among the mutated minigenes may not be disease causing site because we detected no variants from the mRNA extracted from HEK293T cells transfected with mutated minigene except the variants in patients' cDNA. This result suggests that there was a disease-causing site among the polymorphic sites in the wild-type minigene referred to in this study. Further study is needed to identify the disease-causing site.

When we analyzed the function of the mutant protein, we found that the mutant protein cannot function as a normal one to rescue the cells knocking down an endogenous STK11 protein. According to the results from our study, there might be two explanations. One is that the mutation does not influence nuclear distribution of STK11, but it reduces the cytoplasmic location compared to the wild-type. The other is that the kinase domain and no CRD domain of STK11 are defected in the mutant which might influence the function of the STK11 protein. These results indicate that the reduced amount of STK11 in cytoplasm might be not enough to well perform the function even if the mutants have partial functions of wild-type STK11, which is another molecular mechanism of the c.921-2 A>C variation causing PJS in the patients.

In summary, we reported a novel variation in intron 7 of the *STK11* gene which could generate aberrant transcripts in the patients and confirmed this mutation is a PJS-causative mutation. The *STK11* c.921-2 A>C variation may provide us new insights into the molecular mechanism involved in splicing defects underlying PJS. Our findings extend the mutation spectrum of *STK11* mutations and emphasize the biological significance of splice acceptor sites in the context of disease-causing splicing variations.

ETHICAL COMPLIANCE

This study was approved by the Ethics Committees of Shanxi Medical University and written informed consent was obtained from all patients participating in the study.

ACKNOWLEDGMENTS

We thank all patients and family members for their participation in this study, and Ms. Yue Kang from the Chinese Institute for Radiation Protection for assistance in immunohistochemistry. This work was supported by funds from the Shanxi “1331 Project” Collaborative Innovation Center (206541001).

CONFLICT OF INTEREST

The authors have declared no conflict of interest.

DATA AVAILABILITY STATEMENT

The novel variant (c.921-2 A>C) in the STK11 gene was submitted to ClinVar (<https://www.ncbi.nlm.nih.gov/clinvar/>) with accession number VCV000440861.1.

ORCID

Ping Li  <https://orcid.org/0000-0002-6137-6154>

REFERENCES

- Alhopuro, P., Katajisto, P., Lehtonen, R., Ylisaukko-Oja, S. K., Naatsaari, L., Karhu, A., & Launonen, V. (2005). Mutation analysis of three genes encoding novel LKB1-interacting proteins, BRG1, STRADalpha, and MO25alpha, Peutz-Jeghers Syndrome. *British Journal of Cancer*, *92*(6), 1126–1129. <https://doi.org/10.1038/sj.bjc.6602454>
- Chen, J.-H., Zheng, J.-J., Guo, Q., Liu, C., Luo, B., Tang, S.-B., Cheng, J.-D., & Huang, E.-W. (2017). A novel mutation in the STK11 gene causes heritable Peutz-Jeghers syndrome – a case report. *BMC Medical Genetics*, *18*(1), 19. <https://doi.org/10.1186/s12881-017-0373-z>
- Cooper, T. A. (2005). Use of minigene systems to dissect alternative splicing elements. *Methods*, *37*(4), 331–340. <https://doi.org/10.1016/j.ymeth.2005.07.015>
- de Leng, W. W., Jansen, M., Carvalho, R., Polak, M., Musler, A. R., Milne, A. N., & Offerhaus, G. J. (2007). Genetic defects underlying Peutz-Jeghers syndrome (PJS) and exclusion of the polarity-associated MARK/Par1 gene family as potential PJS candidates. *Clinical Genetics*, *72*(6), 568–573. <https://doi.org/10.1111/j.1399-0004.2007.00907.x>
- Hanks, S. K., Quinn, A. M., & Hunter, T. (1988). The protein kinase family: Conserved features and deduced phylogeny of the catalytic domains. *Science*, *241*(4861), 42–52. <https://doi.org/10.1126/science.3291115>
- Hardie, D. G., & Carling, D. (1997). The AMP-activated protein kinase—fuel gauge of the mammalian cell? *European Journal of Biochemistry*, *246*(2), 259–273. <https://doi.org/10.1111/j.1432-1033.1997.00259.x>
- Hastings, M. L., Resta, N., Traum, D., Stella, A., Guanti, G., & Krainer, A. R. (2005). An LKB1 AT-AC intron mutation causes Peutz-Jeghers syndrome via splicing at noncanonical cryptic splice sites. *Nature Structural & Molecular Biology*, *12*(1), 54–59. <https://doi.org/10.1038/nsmb873>
- Hawley, S. A., Boudeau, J., Reid, J. L., Mustard, K. J., Udd, L., Makela, T. P., & Hardie, D. G. (2003). Complexes between the LKB1 tumor suppressor, STRAD alpha/beta and MO25 alpha/beta are upstream kinases in the AMP-activated protein kinase cascade. *Journal of Biology*, *2*(4), 28. <https://doi.org/10.1186/1475-4924-2-28>
- Hearle, N., Schumacher, V., Menko, F. H., Olschwang, S., Boardman, L. A., Gille, J. J. P., Keller, J. J., Westerman, A. M., Scott, R. J., Lim, W., Trimbath, J. D., Giardiello, F. M., Gruber, S. B., Offerhaus, G. J. A., de Rooij, F. W. M., Wilson, J. H. P., Hansmann, A., Möslein, G., Royer-Pokora, B., ... Houlston, R. S. (2006). Frequency and spectrum of cancers in the Peutz-Jeghers syndrome. *Clinical Cancer Research*, *12*(10), 3209–3215. <https://doi.org/10.1158/1078-0432.ccr-06-0083>
- Hemminki, A., Markie, D., Tomlinson, I., Avizienyte, E., Roth, S., Loukola, A., & Aaltonen, L. A. (1998). A serine/threonine kinase gene defective in Peutz-Jegheus syndrome. *Nature*, *391*(6663), 184–187.
- Hemminki, A., Tomlinson, I., Markie, D., Järvinen, H., Sistonen, P., Björkqvist, A.-M., Knuutila, S., Salovaara, R., Bodmer, W., Shibata, D., Chapelle, A. D. L., & Aaltonen, L. A. (1997). Localization of a susceptibility locus for Peutz-Jeghers syndrome to 19p using comparative genomic hybridization and targeted linkage analysis. *Nature Genetics*, *15*(1), 87–90. <https://doi.org/10.1038/ng0197-87>
- Hong, S. P., Leiper, F. C., Woods, A., Carling, D., & Carlson, M. (2003). Activation of yeast Snf1 and mammalian AMP-activated protein kinase by upstream kinases. *Proceedings of the National Academy of Sciences of the United States of America*, *100*(15), 8839–8843. <https://doi.org/10.1073/pnas.1533136100>
- Huang, Z. H., Miao, S. J., Wang, L., Zhang, P., Wu, B. B., Wu, J., & Huang, Y. (2015). Clinical characteristics and STK11 gene mutations in Chinese children with Peutz-Jeghers syndrome. *BMC Gastroenterology*, *15*, 8. <https://doi.org/10.1186/s12876-015-0397-9>
- Jenne, D. E., Reomann, H., Nezu, J.-I., Friedel, W., Löff, S., Jeschke, R., Müller, O., Back, W., & Zimmer, M. (1998). Peutz-Jeghers syndrome is caused by mutations in a novel serine threonine kinase. *Nature Genetics*, *18*(1), 38–43. <https://doi.org/10.1038/ng0198-38>
- Kottakis, F., Nicolay, B. N., Roumane, A., Karnik, R., Gu, H., Nagle, J. M., Boukhali, M., Hayward, M. C., Li, Y. Y., Chen, T., Liesa, M., Hammerman, P. S., Wong, K. K., Hayes, D. N., Shirihai, O. S., Dyson, N. J., Haas, W., Meissner, A., & Bardeesy, N. (2016). LKB1 loss links serine metabolism to DNA methylation and tumorigenesis. *Nature*, *539*(7629), 390–395. <https://doi.org/10.1038/nature20132>
- Kuragaki, C., Enomoto, T., Ueno, Y., Sun, H., Fujita, M., Nakashima, R., Ueda, Y., Wada, H., Murata, Y., Toki, T., Konishi, I., & Fujii, S. (2003). Mutations in the STK11 gene characterize minimal deviation adenocarcinoma of the uterine cervix. *Laboratory Investigation*, *83*(1), 35–45. <https://doi.org/10.1097/01.LAB.0000049821.16698.D0>
- Li, P., Zhang, L., Zhao, N., Xiong, Q., Zhou, Y. A., Wu, C., & Xiao, H. (2019). A novel alpha-galactosidase A splicing mutation predisposes to Fabry disease. *Frontiers in Genetics*, *10*, 60. <https://doi.org/10.3389/fgene.2019.00060>
- Lizcano, J. M., Göransson, O., Toth, R., Deak, M., Morrice, N. A., Boudeau, J., Hawley, S. A., Udd, L., Mäkelä, T. P., Hardie, D. G., & Alessi, D. R. (2004). LKB1 is a master kinase that activates 13 kinases of the AMPK subfamily, including MARK/PAR-1. *The EMBO Journal*, *23*(4), 833–843. <https://doi.org/10.1038/sj.emboj.7600110>

- Masuda, K., Kobayashi, Y., Kimura, T., Umene, K., Misu, K., Nomura, H., Hirasawa, A., Banno, K., Kosaki, K., Aoki, D., & Sugano, K. (2016). Characterization of the STK11 splicing variant as a normal splicing isomer in a patient with Peutz-Jeghers syndrome harboring genomic deletion of the STK11 gene. *Human Genome Variation*, 3, 16002. <https://doi.org/10.1038/hgv.2016.2>
- Mehenni, H., Resta, N., Park, J. G., Miyaki, M., Guanti, G., & Costanza, M. C. (2006). Cancer risks in LKB1 germline mutation carriers. *Gut*, 55(7), 984–990. <https://doi.org/10.1136/gut.2005.082990>
- Peña, C. G., Nakada, Y., Saatcioglu, H. D., Aloisio, G. M., Cuevas, I., Zhang, S., Miller, D. S., Lea, J. S., Wong, K.-K., DeBerardinis, R. J., Amelio, A. L., Brekken, R. A., & Castrillon, D. H. (2015). LKB1 loss promotes endometrial cancer progression via CCL2-dependent macrophage recruitment. *Journal of Clinical Investigation*, 125(11), 4063–4076. <https://doi.org/10.1172/jci82152>
- Shackelford, D. B., & Shaw, R. J. (2009). The LKB1-AMPK pathway: Metabolism and growth control in tumour suppression. *Nature Reviews Cancer*, 9(8), 563–575. <https://doi.org/10.1038/nrc2676>
- Shorning, B. Y., & Clarke, A. R. (2016). Energy sensing and cancer: LKB1 function and lessons learnt from Peutz-Jeghers syndrome. *Seminars in Cell & Developmental Biology*, 52, 21–29. <https://doi.org/10.1016/j.semcdb.2016.02.015>
- Utsunomiya, J., Gocho, H., Miyanaga, T., Hamaguchi, E., & Kashimura, A. (1975). Peutz-Jeghers syndrome: its natural course and management. *The Johns Hopkins Medical Journal*, 136(2), 71–82.
- van Lier, M. G., Wagner, A., Mathus-Vliegen, E. M., Kuipers, E. J., Steyerberg, E. W., & van Leerdam, M. E. (2010). High cancer risk in Peutz-Jeghers syndrome: a systematic review and surveillance recommendations. *American Journal of Gastroenterology*, 105(6), 1258–1264. author reply 1265. <https://doi.org/10.1038/ajg.2009.725>
- Westerman, A. M., Entius, M. M., Boor, P. P., Koole, R., de Baar, E., Offerhaus, G. J., & Wilson, J. H. (1999). Novel mutations in the LKB1/STK11 gene in Dutch Peutz-Jeghers families. *Human Mutation*, 13(6), 476–481. [https://doi.org/10.1002/\(sici\)1098-1004\(1999\)13:6<476:aid-humu7>3.0.co;2-2](https://doi.org/10.1002/(sici)1098-1004(1999)13:6<476:aid-humu7>3.0.co;2-2)
- Westerman, A. M., Entius, M. M., de Baar, E., Boor, P. P., Koole, R., van Velthuysen, M. L., & Wilson, J. H. (1999). Peutz-Jeghers syndrome: 78-year follow-up of the original family. *Lancet*, 353(9160), 1211–1215.
- Woods, A., Johnstone, S. R., Dickerson, K., Leiper, F. C., Fryer, L. G. D., Neumann, D., Schlattner, U., Wallimann, T., Carlson, M., & Carling, D. (2003). LKB1 is the upstream kinase in the AMP-activated protein kinase cascade. *Current Biology*, 13(22), 2004–2008. <https://doi.org/10.1016/j.cub.2003.10.031>
- Yoo, L. I., Chung, D. C., & Yuan, J. Y. (2002). LKB1 – A master tumour suppressor of the small intestine and beyond. *Nature Reviews Cancer*, 2(7), 529–535. <https://doi.org/10.1038/nrc843>

SUPPORTING INFORMATION

Additional Supporting Information may be found online in the Supporting Information section.

How to cite this article: Zhao, N., Wu, H., Li, P., Wang, Y., Dong, L., Xiao, H., & Wu, C. (2021). A novel pathogenic splice site variation in *STK11* gene results in Peutz-Jeghers syndrome. *Molecular Genetics & Genomic Medicine*, 9, e1729. <https://doi.org/10.1002/mgg3.1729>